

HARMONIC ANALYSIS AND MODELLING OF MAGNETISATION PROCESS IN SOFT FERROMAGNETIC MATERIAL *

**Branko Koprivica¹, Ioan Dumitru²,
Alenka Milovanović¹, Ovidiu Caltun²**

¹University of Kragujevac, Faculty of Technical Sciences Čačak, Čačak, Serbia

²Ioan Cuza University of Iasi, Faculty of Physics, Iasi, Romania

Abstract. *The aim of this paper is to present a research of magnetic hysteresis loops of a toroidal ferromagnetic core made of electrical steel. The experimental results of induced voltage, magnetic induction and hysteresis loop obtained at different frequencies of the sinusoidal excitation magnetic field have been presented. The harmonic content of the induced voltage and magnetic induction have been calculated using Fast Fourier Transformation. Observed variation of higher harmonics with frequency has been correlated to the mechanism of magnetic domain walls damping. A variation of harmonics of the magnetic induction with the amplitude of the excitation magnetic field has been analysed and a proper mathematical model has been proposed. Furthermore, the influence of the triangularly shaped excitation magnetic field and the distorted shape excitation that produces sinusoidal induction on the shape of hysteresis loop and harmonic content of the induced voltage and the magnetic induction has been analysed and discussed.*

Key words: *Ferromagnetic core, FFT and harmonic analysis, magnetic hysteresis, sinusoidal and triangular excitation magnetic field, sinusoidal induction*

1. INTRODUCTION

Measurement and modelling of the dynamic magnetisation process in the electrical steel are subject of interest for many years. It reaches its culmination in the last decay through the development of sophisticated measurement setups, such as the one presented in [2], as well as in the comprehensive modelling approaches and techniques of analysis of this process under various amplitudes, frequencies and types of excitation [3-6].

Received May 23, 2016; received in revised form July 13, 2016

Corresponding author: Branko Koprivica

University of Kragujevac, Faculty of Technical Sciences, Svetog Save 65, 32000 Čačak, Serbia

(E-mail: branko.koprivica@ftn.kg.ac.rs)

*An earlier version of this paper was presented at the 12th International Conference on Applied Electromagnetics (IIEC 2015), August 31 - September 02, 2015, in Niš, Serbia [1].

The analysis of higher harmonics induced in AC circuits systematic attracted the attention of researchers because it has two equally important aspects. One is related to the modelling of the magnetic hysteresis [7, 8]. The second aspect relates to the theoretical perspective focused on higher frequencies and magnetisation processes in magnetic materials [9]. Even proved to be a powerful tool, such analysis is not so much used by researchers in the field of electrical steel industrial application. Therefore, this paper is focused on the comprehensive investigation of the magnetic hysteresis shape and harmonic analysis of induced signals in electrical steel cores.

The measurements have been done on the toroidal core sample using classical oscilloscope based method [10]. An application designed and implemented in LabVIEW software has been used for calculation of all quantities of interest [11].

The magnetisation process and consequently hysteresis loops have been studied at different amplitudes and frequencies of the sinusoidal excitation magnetic field. The induced voltage and the magnetic induction waveforms obtained from measurements have been analysed and represented in the frequency domain by using fast Fourier transform. A variation of the harmonic content of these signals at different amplitudes and frequencies of the sinusoidal excitation field has been computed, analysed and interpreted in terms of magnetic domains damping. A proper mathematical model of this variation has been proposed. This model comprises the variation of higher harmonic amplitudes as well as the variation of their initial phases.

Furthermore, a triangular shape of the excitation magnetic field has been also used in some measurements in order to examine the influence of the magnetic field rate to the magnetisation process and core response at different excitation waveform. Also, the harmonic contents of the induced voltage and the magnetic induction in this case have been presented. Also, similar analysis has been made in the case of the distorted excitation that produces sinusoidal induction.

The practical impact of the results presented should be mostly on the researchers in the field of electrical engineering in proper understanding of the dynamic magnetisation process in the electrical steel from the physical point of view. Its practical uses may be in the development of novel approaches of inclusion of magnetic hysteresis in the modelling of magnetic cores of electrical machines, power transformer and different kind of electronic parts. Also, they may be used in the analysis of power loss and efficiency of such equipment.

2. EXPERIMENTAL SETUP

In Fig. 1 is schematically represented the experimental setup. On a toroidal core, made of electrical steel, primary and secondary coils with the same number of turns were wounded. The primary winding having has been connected in series with a power source and a non-inductive resistor R . The voltage u_1 across the resistor R and voltage u_2 induced in the secondary winding have been connected to the input channels of the digital oscilloscope interconnected with the computer via GPIB interface in order to record the signals.

The magnetic field H and the magnetic induction B have been calculated from the measured data using expressions (1) and (2) [11]:

$$H = \frac{N_1 u_1}{l R}, \quad (1)$$

$$B = \frac{1}{N_2 S} \int_0^t u_2 dt, \quad (2)$$

where N_1 and N_2 are the number of the turns in the primary and secondary winding, l is the effective length of the magnetic circuit and S is its cross-section area. Measured data have been processed using a LabVIEW application in order to represent the hysteresis loop and harmonics of induced signal.

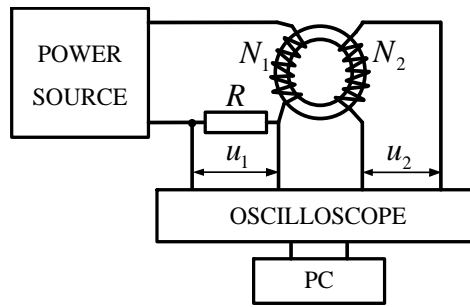


Fig. 1 Experimental setup

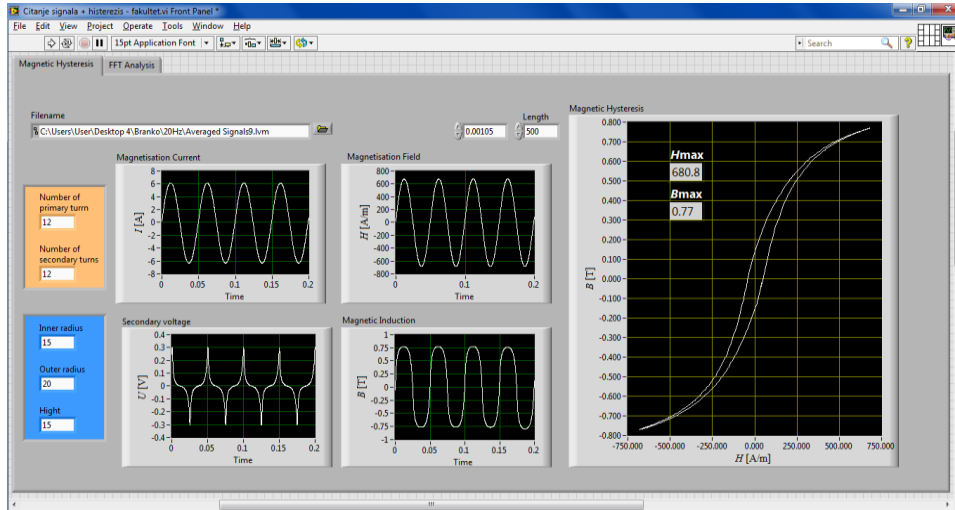
3. LABVIEW APPLICATION – HYSTERESIS REPRESENTATION AND FFT ANALYSIS

A simple LabVIEW application has been made in order to process the measurement results. It contains two tabs for results presentation and analysis. The first tab shows an input data, such as the dimensions of the toroidal core and a number of turns in the primary and secondary coil, as well as waveforms of the measured magnetizing current and induced voltage. It also presents the waveforms of the magnetic field and the magnetic induction obtained using (1) and (2), as well as the magnetic hysteresis loop that correspond to these two waveforms, Fig. 2a.

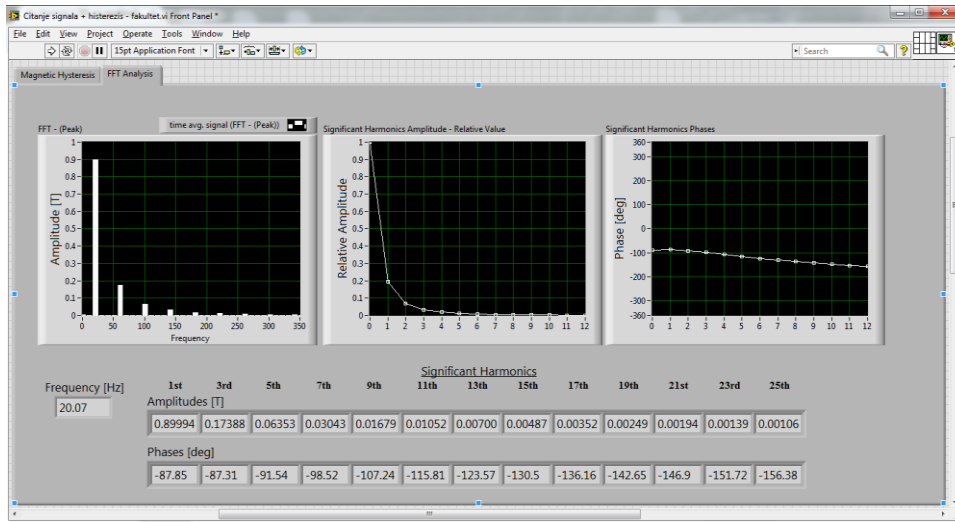
The waveforms of the induced voltage and magnetic induction have been analysed using fast Fourier transform (FFT) and the results obtained are contained in the second tab of LabVIEW application, Fig. 2b. A result of the FFT of the signal $a(t)$ is obtained in the form of two arrays that respectively contain the amplitudes of the harmonic components A_i ($i=0, 1, 2, 3, \dots$) and their initial phases θ_i ($i=0, 1, 2, 3, \dots$). Consequently, a time waveform of the signal $a(t)$ can be approximately represented over the DC component $-A_0$, the first harmonic $-A_1$ and the higher harmonics $-A_i$ ($i=2, 3, 4, \dots$) using the equation (3):

$$\begin{aligned} a(t) &= \sum_{i=0}^N A_i \cos[2\pi i f t + \theta_i] = \\ &= A_0 + A_1 \cos[2\pi f t + \theta_1] + A_2 \cos[4\pi f t + \theta_2] + \dots + A_N \cos[2N\pi f t + \theta_N], \end{aligned} \quad (3)$$

where N is the number of used harmonic components and f is the frequency of the first harmonic (fundamental frequency). In this paper, analysed waveforms are periodic functions of time symmetrical with respect to the time axis. Therefore, their FFT contains only odd harmonics (as presented in Fig. 2b) and they have significant values and importance in the analysis.



a)



b)

Fig. 2 LabVIEW application: a) first tab, b) second tab

4. EXPERIMENTAL RESULTS

Most of the experimental results presented in this paper have been obtained using sinusoidal excitation magnetic field. During the measurements the amplitude and the frequency of this field has been varied. A total number of six sets of measurements at different frequencies (20 Hz, 30 Hz, 40 Hz, 50 Hz, 93 Hz and 141 Hz) have been performed. During the each set the amplitude of the excitation magnetic field has been varied in ten steps, from low value (beginning of the sample magnetisation) to the high value that corresponds to the magnetic saturation of the sample. Some of these measurement results have been presented in this section of the paper, while the results of the FFT analysis performed on all measurement results have been presented in the next section.

Fig. 3a presents waveforms of the secondary voltage induced at different amplitudes of the sinusoidal excitation magnetic field at 50 Hz. A family of hysteresis loops obtained at sinusoidal excitation magnetic field at 50 Hz is presented in Fig. 3b.

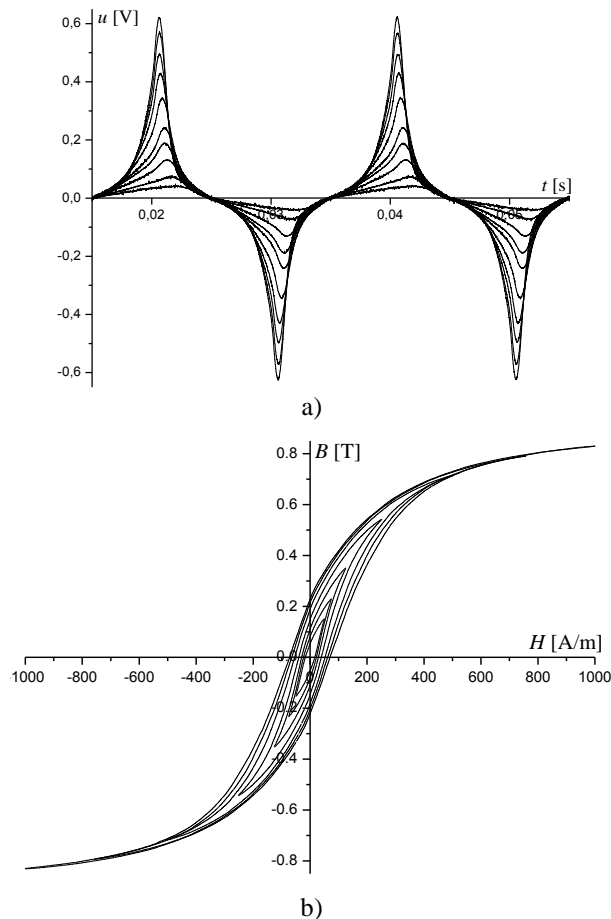


Fig. 3 Sinusoidal excitation at 50 Hz: a) waveforms of induced voltage, b) family of hysteresis loops at 50 Hz - sinusoidal excitation

A comparison of hysteresis loops obtained at different frequencies (20 Hz to 141 Hz) of the sinusoidal magnetic field excitation is presented in Fig. 4. It is evident that the shape of the loops is highly dependent on the frequency of the excitation field. Obviously, larger frequency means wider hysteresis loop that is associated with higher power loss due to the increase of the eddy currents and the magnetic viscosity of domain wall movement [12, 13].

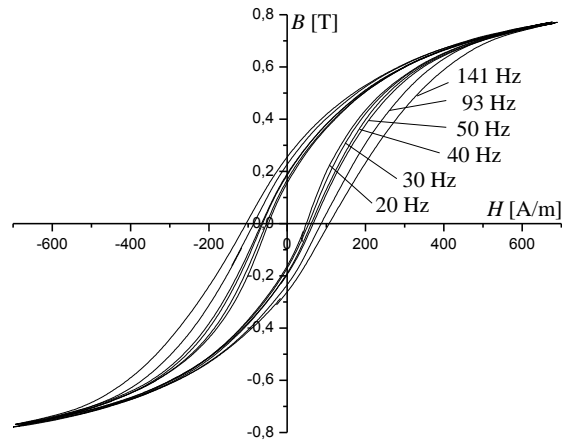


Fig. 4 Hysteresis loop shape at different frequencies of sinusoidal excitation

5. RESULTS OF FFT ANALYSIS

Fig. 5a shows normalized values of the first and higher odd harmonics V_i/V_1 , $i = 1, 3, \dots, 25$, (only odd harmonics have significant value) of the induced voltage at various amplitudes of 50 Hz sinusoidal excitation. Corresponding normalized odd harmonic components of the magnetic induction B_i/B_1 , $i = 1, 3, \dots, 25$, are presented in Fig. 5b.

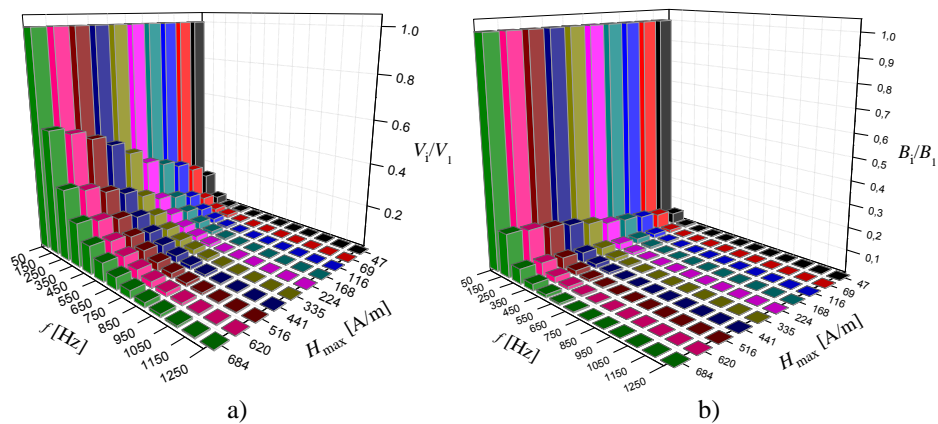


Fig. 5 Harmonics of: a) induced voltage, b) magnetic induction, at 50 Hz - sinusoidal excitation

As expected, the results presented in Fig. 5a have confirmed highly distorted shape (from sinusoidal) of the induced voltage. The presence of higher harmonics has been observed even at low excitation magnetic field while at higher excitations (close to the magnetic saturation) the 19th and 21st harmonics have significant value (around 1 % of the first harmonic).

The harmonic content of the magnetic induction is notably different from the induced voltage harmonic content, Fig. 5b. In this case, only harmonics up to 11th have significant value (larger than 1% of the first harmonic). Even so, the magnetic induction is highly distorted from the sinusoidal waveform.

Fig. 6 shows normalized values of the first and higher harmonics of the secondary voltage induced at different frequencies of the excitation magnetic field with amplitude of 210 A/m, 430 A/m and 680 A/m.

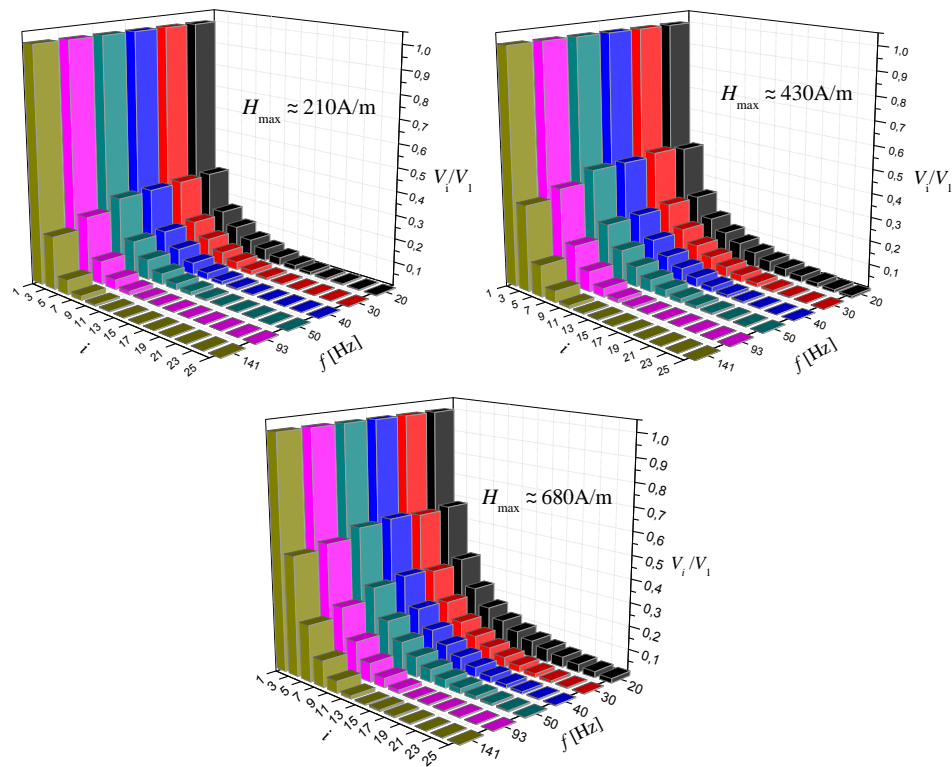


Fig. 6 Harmonics of induced voltage, at different frequencies and amplitudes - sinusoidal excitation

From these results can be observed that the normalized amplitudes of the harmonics at frequencies up to 50 Hz do not change significantly regardless of the excitation field, while at double of frequency suppression of the harmonics is evident. At low frequencies both domain wall movement and magnetisation rotation contribute to the magnetisation process. At high frequencies the domain wall movements are strongly damped by eddy currents and magnetisation rotation dominates the process [9, 14].

Domain wall motion in bulk metallic samples is dominated by eddy currents that produce power loss and limit the mobility of domain walls [9, 14]. Eddy currents can be calculated from Maxwell's equations, as well as power loss they produce. The effect of the induced eddy field is a decrease of the magnetic field inside material because it has a direction opposite to the direction of the excitation field. Thus, due to the decrease of the magnetic field the average wall velocity is also decreasing. Also, a number of domains and domain walls can be greater in this case. Domain wall motion induces microcurrents at a microstructural level and causes power loss (excess eddy current loss). Therefore, at higher frequencies, with a higher number of domain walls, higher power loss occurs. Altogether, a total power loss in the material will increase with the frequency due to the increase of these two components of power loss. Eddy current effects, consequently power loss, can be reduced by the decrease of the material thickness and its conductivity (this will reduce induced eddy currents) and by domain refining which will reduce microcurrents produced by domain wall motion [12, 14].

6. MODELLING BY USING FFT

The normalized harmonics of the magnetic induction B_i/B_1 , $i=1, 3, \dots, 11$ and their normalized initial phases θ_i/θ_1 , $i=1, 3, \dots, 11$ obtained at 20 Hz for various amplitudes of the sinusoidal excitation magnetic field are presented in Fig. 7a. Variation of normalized harmonics of magnetic induction B_i/B_1 , $i=1, 3, \dots, 11$ obtained at different frequencies of the sinusoidal excitation magnetic field with amplitude of 680 A/m is presented in Fig. 7b. According to these results, only harmonics up to 11th have significant value in comparison to the first harmonic (higher than 1 % of the first harmonic). Therefore, only these harmonics have been used in the further analysis. Also, a suppression of the higher harmonics can be observed at higher excitation frequencies, such as 93 Hz and 141 Hz, Fig. 7b, while at lower frequencies such variation is negligible.

An analysis of a variation of the normalized amplitudes and initial phases of harmonic components has been performed. It has been noticed that this variation can be approximately expressed as follows:

$$\frac{B_i}{B_1} = a e^{bi + \frac{c}{i}}, \quad (4)$$

$$\frac{\theta_i}{\theta_1} = d i^2 + 1, \quad (5)$$

where i is the order of the odd harmonic component and a , b , c and d are fitting parameters. A comparison of normalized amplitudes and initial phases of magnetic induction harmonic components, up to 11th, obtained by using FFT and by using expressions (4) and (5) is presented in Fig. 8. Some difference between the results obtained can be observed, at the acceptable level.

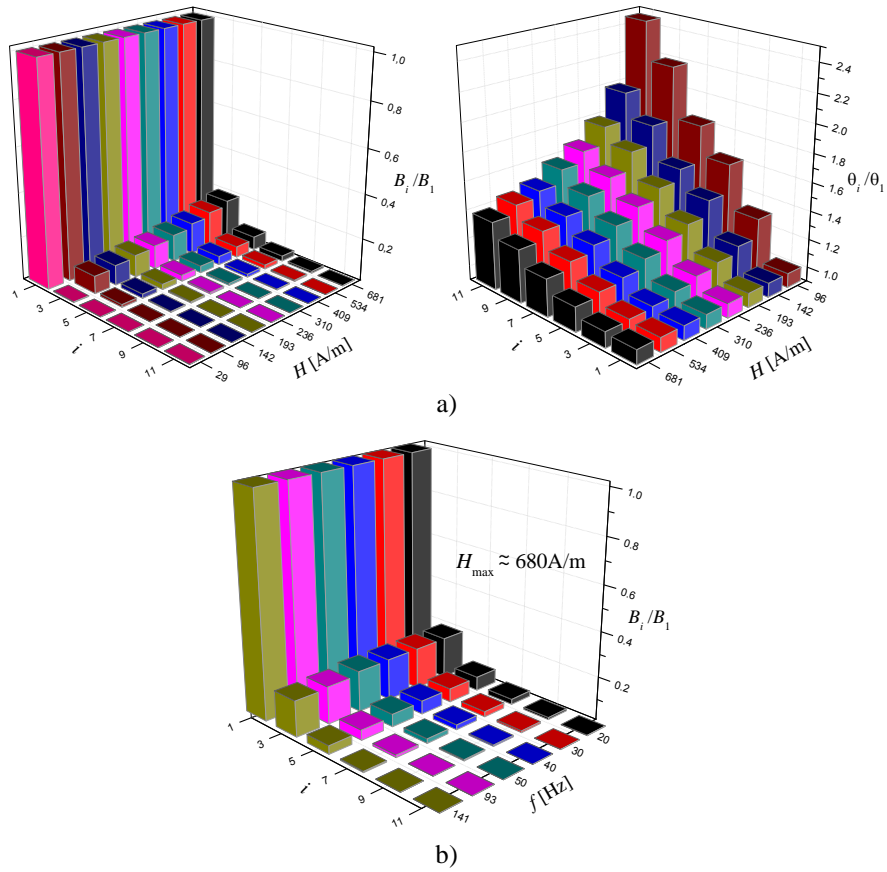


Fig. 7 a) Harmonics of magnetic induction and their initial phases, for different amplitudes of sinusoidal excitation, at 20 Hz, b) Harmonics of magnetic induction for different frequencies of sinusoidal excitation

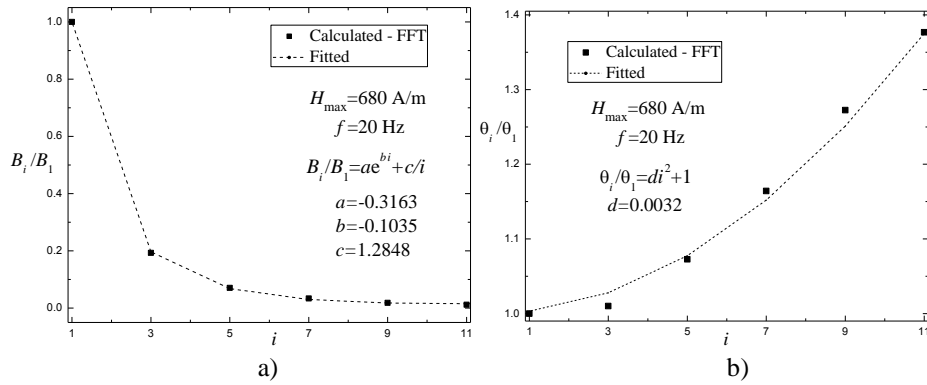


Fig. 8 Comparison of: a) normalized amplitudes and b) normalized initial phases, of the harmonic components of magnetic induction obtained using FFT and fitting function

For certain amplitude of the excitation magnetic field parameters a , b , c and d are constant, but their values vary with the change of the magnetic field. These variations have been presented in Fig. 9.

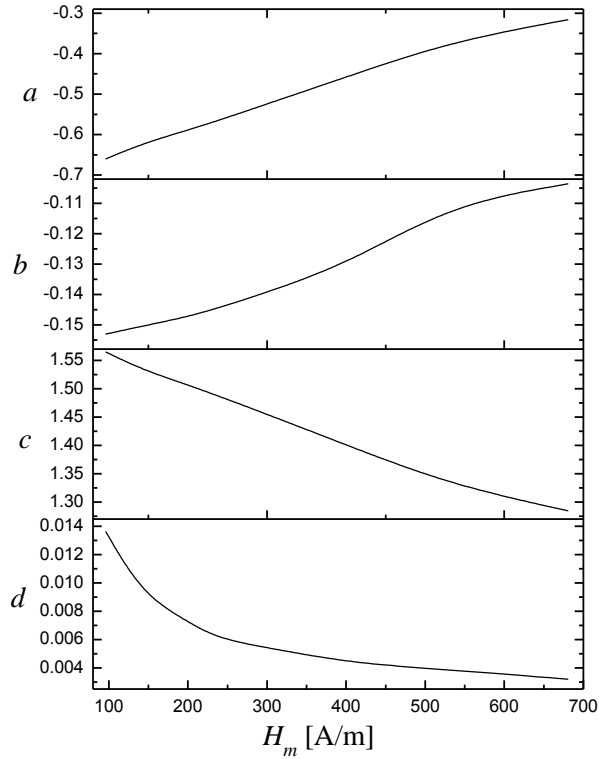


Fig. 9 Variation of fitting parameters a , b , c and d with the amplitude of the excitation magnetic field

Expressions (4) and (5) give normalized values of amplitudes and initial phases, but for further calculations it is needed to know also values of B_1 and θ_1 . It has been found that these two quantities amount approximately $B_1=0.9$ T and $\theta_1=\pi/2$. Accordingly, magnetic induction can be expressed as:

$$B(t) = B_1 \sum_{i=1}^{11} \left(a e^{bi} + \frac{c}{i} \right) \cos[2\pi i f t + \theta_1 (d i^2 + 1)]; \quad i = 1, 3, \dots, 11. \quad (6)$$

A time waveform of induction can be obtained using this expression. It can be further used in modelling of the magnetic hysteresis, along with the sinusoidal excitation magnetic field as input waveform. A comparison of the measured and modelled hysteresis loop has been presented in Fig. 10.

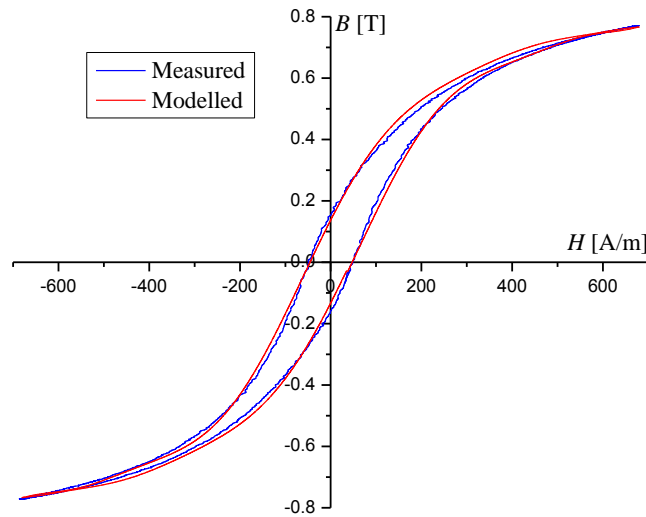


Fig. 10 Comparison of measured and modelled hysteresis loop, at 20 Hz

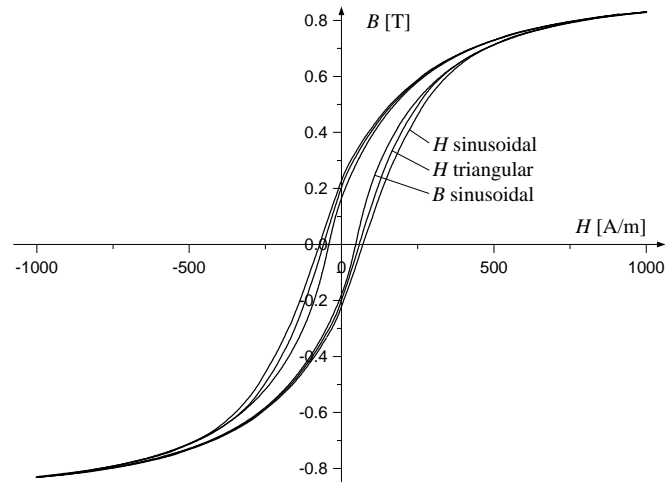
7. HYSTERESIS LOOP AT VARIOUS EXCITATION WAVEFORMS

A shape of the magnetic hysteresis loop strongly depends on the shape of the excitation magnetic field (magnetic induction) [15 - 17]. Such behaviour has also been observed during the measurements with the used toroidal sample made of electrical steel. A comparison of hysteresis loops obtained with sinusoidal and triangular excitation field and sinusoidal induction (at 50 Hz) is presented in Fig. 11a.

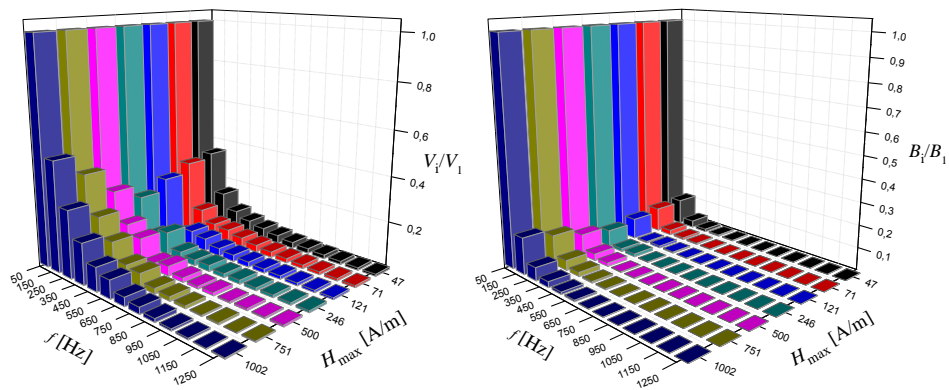
It is evident that sinusoidal excitation produces widest hysteresis loop, while narrowest loop is obtained at sinusoidal induction. In this case, of three excitation fields with the same frequency but different in shape, the difference in shape corresponds to different magnetic field rate and the response of the material is different. It is important to analyze the response of the material under triangular excitation from the physical point of view, since it gives information about the real characteristics of the ferromagnetic material. On the other hand, proper understanding of the magnetisation process obtained under sinusoidal induction is very important in the electrical engineering and electronics.

This can be explained by means of the difference in the harmonic content of the excitation fields. While sinusoidal excitation contains only first harmonic, triangular excitation contains also higher harmonic (3rd, 5th, 7th and 9th harmonic in the percentage of 11.12 %, 4.01 %, 2.05 % and 1.24 % of the first harmonic, respectively) which significantly influence the harmonic content of the induces signal and the magnetic induction, Fig. 11b. The distribution of the harmonics shown in this figure is significantly different from the distribution presented in Fig. 5. Also, the suppression of all higher harmonics can be observed in Fig. 11b. These two excitations produce non-sinusoidal magnetic induction, while in the third case the excitation is such that the magnetic induction is sinusoidal. As in the case of the triangular excitation, it also contains higher harmonics that in this case completely suppress all higher harmonics in the induced voltage and the magnetic induction. Observed difference

can be also analysed in another sense. Beside differences in the harmonic content, all three excitation fields of the same frequency have different rate of change (dH/dt).



a)



b)

Fig. 11 a) Hysteresis loops comparison at 50 Hz sinusoidal and triangular excitation magnetic field and sinusoidal magnetic induction, b) Harmonics of induced voltage and magnetic induction, at 50 Hz triangular excitation

Corresponding waveforms of the magnetic field and induction and magnetic field rate of change in time in these cases are presented in Fig. 12. Three waveforms of the excitation magnetic field are aligned so that their maximums appear at 0.05 s and all other waveforms are given synchronously to these three waveforms, as they appear during the measurement. Thus, the rate of change of triangular excitation is constant during one quarter of the period, while sinusoidal excitation has a variable rate of change, as well as the excitation that gives sinusoidal induction (this one will be called distorted excitation in the further analysis). It is interesting to analyze how these differences influence the shape of the magnetic induction

waveform. Since the corresponding hysteresis loops, Fig. 11a, have only one common point, the saturation point, it is most convenient to observe changes in the waveforms after reaching this point. As shown in Fig. 12, all three excitation fields are at the maximum at 0.05 s

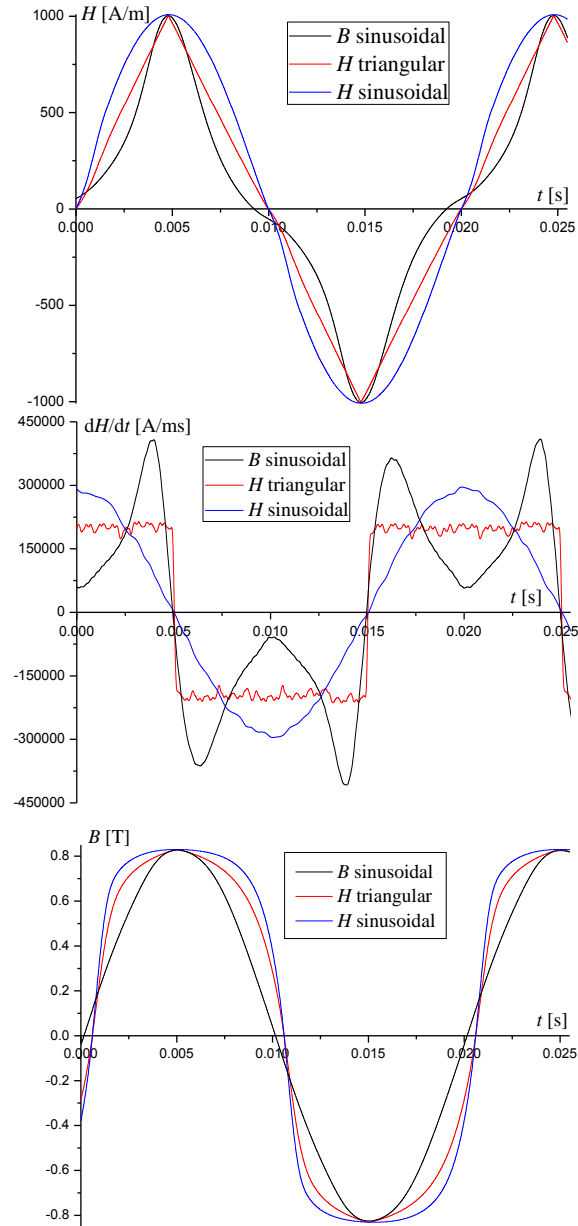


Fig. 12 Magnetic field, field rate of change and induction waveforms, sinusoidal and triangular excitation magnetic field and sinusoidal magnetic induction, at 50 Hz

and after that moment they start to decrease with the different rate of change. It can be observed that sinusoidal excitation field decrease much slower than other two excitation fields, with the sinusoidal rate of change. Triangular excitation reaches quickly its minimum rate of change (fastest change in the decreasing direction), while distorted excitation almost follows the triangular for some short period of time and after that period quickly reaches its minimum rate of change. Consequently, the magnetic induction of the triangular and distorted excitation matches each other for some short period of time. After that period the magnetic induction of the distorted excitation decreases rapidly, much faster than other two magnetic inductions, even the rate of change of the excitation varies. Since the rate of change of the sinusoidal excitation is much lower during that period, the corresponding magnetic induction is decreasing much slower than other two inductions. At 0.075 s all three excitations are at the different level, as well as the corresponding inductions, while their rates of change are at the same level. During this period, from 0.05 s to 0.075 s, the rotation of the magnetic domains is the dominant process in the material and domain wall movement is not so significant [15]. The response of the material (change in the magnetic induction) during this process is such that it strictly follows the variation of the excitation magnetic field. Therefore, fastest change of the excitation produces fastest response.

After 0.075 s the distorted excitation starts to change slower than other two excitations, while the sinusoidal excitation has the fastest variation. Very soon the magnetic induction at the triangular and sinusoidal excitation starts to decrease rapidly, much faster than the magnetic induction of the distorted excitation. This corresponds to the increase of the retrieval of the domain walls and the increase of number of domains. Also, misalignment of the magnetic moment of domains with the excitation magnetic field becomes larger.

At the moment when the excitation field becomes zero the remanent magnetisation in the material is present. The level of the remanence depends on the previous magnetisation process in the material. In the previously analysed processes, lower level of the remanence corresponds to the higher rate of change of the excitation magnetic field starting from the saturation. Consequently, lower remanence corresponds to lower coercive magnetic field, as it can be observed in Fig. 11a.

After reaching the coercivity point, the magnetisation process can be analysed in the same way as it has been previously described.

8. CONCLUSION

This paper addressed the influence of magnetic field amplitude and excitation frequency on the shape of hysteresis loop of the toroidal core sample made of electrical steel. Also, a comparison of the hysteresis loops at sinusoidal and triangular waveform of the excitation field has been made, as well as at the excitation that produces sinusoidal excitation.

The harmonic content of the induced voltage in the secondary coil of the transformer and of magnetic induction at different frequency is dependent on the magnetisation processes. A suppression of the higher harmonics in the induced voltage and the magnetic induction has been observed at higher frequencies of the excitation field. This behaviour has been related to the domain walls damping.

An analysis of a variation of normalized amplitudes and initial phases of harmonic components has been performed and a proper mathematical model has been proposed. Also, a variation of the model parameters with the excitation magnetic field has been presented.

Presented results have importance in proper understanding of the dynamic magnetisation process in the electrical steel. Also, these results can be useful in the modelling of the magnetic hysteresis. Future research will be focused on the influence of the frequency and the shape of the excitation field on power loss in the material and its modelling.

Acknowledgement: Ioan Dumitru acknowledges the support given by Romanian CNCS-UEFISCDI under project PN-II-RU-TE-2012-3-0449. Also, Branko Koprivica and Alenka Milovanovic acknowledge that this work was supported by the Ministry of Education, Science and Technological Development of the Republic of Serbia, Grant No. TR33016.

REFERENCES

- [1] B. Koprivica, I. Dumitru, A. Milovanovic, O. Caltun, "Harmonic analysis of induced signal in magnetisation process of toroidal ferromagnetic core", In Proceedings of the Extended Abstracts of the 12th International Conference on Applied Electromagnetics (IEEC 2015), Niš, Serbia, 2015, pp. 53-55.
- [2] S. Zurek, P. Marketos, T. Meydan, A.J. Moses: "Use of Novel Adaptive Digital Feedback for Magnetic Measurements Under Controlled Magnetizing Conditions", *IEEE Transactions on Magnetics*, vol. 41, no. 11, pp. 4242-4249, Nov. 2005.
- [3] A. J. Moses, J. Leicht, "Power Loss of Non Oriented Electrical Steel Under Square Wave Excitation", *IEEE Transactions on Magnetics*, vol. 37, no. 4, pp. 2737-2739, July 2001.
- [4] E. Barbisio, F. Fiorillo, C. Ragusa, "Predicting Loss in Magnetic Steels Under Arbitrary Induction Waveform and with Minor Hysteresis Loops", *IEEE Transactions on Magnetics*, vol. 40, no. 4, pp. 1810-1819, July 2004.
- [5] S. E. Zirka, Y. I. Moroz, P. Marketos, A. J. Moses, D. C. Jiles, "Measurement and Modeling of B-H Loops and Losses of High Silicon Nonoriented Steels", *IEEE Transactions on Magnetics*, vol. 42, no. 10, pp. 3177-3179, Oct. 2006.
- [6] S. Steentjes, S. E. Zirka, Y. E. Moroz, E. Y. Moroz, K. Hameyer: "Dynamic Magnetization Model of Nonoriented Steel Sheets", *IEEE Transactions on Magnetics*, vol. 50, no. 4, p. 7300204, April 2014.
- [7] Y. Saito, Y. Kishino, K. Fukushima, S. Hayano, N. Tsuya, "Modeling of magnetization characteristics and faster magnetodynamic field computation", *Journal of Applied Physics*, vol. 63, no. 8, pp. 3174-3178, April 1988.
- [8] J. Takacs, *Mathematics of hysteretic phenomena*, Wiley-VCH, Weinheim, Germany, 2003.
- [9] O. Caltun, "Fourier transform of signal induced in circuits with soft ferrite cores", In Proc. of the International Symposium on Signals, Circuits and Systems, Iasi, Romania, 10-11 July 2003, vol. 2, pp. 665-668.
- [10] O. Caltun, A. Stancu, P. Andrei, "Experimental method and software for complex characterization of magnetic materials", In Proc. of the 3rd International Conference on Materials for Advanced Technologies – Symposium R – Electromagnetic Materials, Singapore, 3–8 July 2005, pp. 223-226.
- [11] B. Koprivica, A. Milovanovic, M. Djekic, "Determination of characteristics of ferromagnetic material using modern data acquisition system", *Serbian Journal of Electrical Engineering*, vol. 6, no. 3, pp. 451-459, Dec. 2009.
- [12] G. Bertotti, *Hysteresis in Magnetism: For Physicists, Materials Scientists and Engineers*, Academic Press, New York, USA, 1998.
- [13] D.C. Jiles, D.L. Atherton, "Theory of ferromagnetic hysteresis", *Journal of Magnetism and Magnetic Materials*, vol. 61, no. 1-2, pp. 48-60, Sept. 1986.
- [14] A. Hubert, R. Schafer, *Magnetic Domains - The Analysis of Magnetic Microstructures*, Springer, Berlin, Germany, 2008.
- [15] M. S. Lancarotte, A. A. Pentead, "Estimation of core losses under sinusoidal or non-sinusoidal induction by analysis of magnetization rate", *IEEE Transaction on Energy Conversion*, vol. 16, no. 2, pp. 174-179, June 2001.

- [16] R. S. Turtelli, M. Antoni, R. Grossinger, S. Hartl, "Influence of the induction $B(t)$ shape on hysteresis and loss measurements of soft magnetic materials", *IEEE Transaction on Magnetics*, vol. 52, no. 2, , p. 2001704, May 2016.
- [17] C.-J. Wu, S.-Y. Lin, S.-C. Chou, C.-Y. Tsai, J.-Y. Yen, "Temperature effects on the magnetic properties of silicon-steel sheets using standardized toroidal frame", *The Scientific World Journal*, vol. 2014, p. 975051, 2014.